iJRASET
International Journal For Research in Applied Science and Engineering Technology

INTERNATIONAL JOURNAL FOR RESEARCH

IN APPLIED SCIENCE & ENGINEERING TECHNOLOGY

Volume: 8 **Issue:** II **Month of publication:** February 2020

DOI: http://doi.org/10.22214/ijraset.2020.2051

www.ijraset.com

Call: 08813907089 | E-mail ID: ijraset@gmail.com

International Journal for Research in Applied Science & Engineering Technology (IJRASET)
ISSN: 2321-9653; IC Value: 45.98; SJ Impact Factor: 7.177
Volume 8 Issue II Feb 2020- Available at www.ijraset.com

FDM for Alumina based Induction Furnace Wall using Cylindrical Coordinate System

Nirajkumar Mehta[1], Meet Patel[2]
[1]*Associate Professor, Institute of Technology and Management Universe, Vadodara, India*
[2]*Graduate Mechanical Engineer, Gujarat Technological University, Ahmedabad, India Graduate Masters of Management for Engineers, Central Queensland University, Melbourne, Victoria, Australia*

Abstract: ***Furnaces are used for melting many materials like cast iron and steel for casting process. In this research paper, we had done Finite Difference Modelling of Induction melting furnace refractory wall made of alumina ramming mass using cylindrical coordinate system. We have divided actual geometry of furnace refractory wall into 14 elements and 24 nodes. We have derived explicit finite difference equations for all 24 nodes. We have calculated temperature distribution and thermal stress distribution for all different nodes with respect to time. We have plotted graphs for maximum temperature v/s time and maximum stress v/s time. We found that results indicate the effect of thermal fatigue in the induction furnace wall for alumina ramming mass. The analysis is very helpful in understanding how thermal fatigue failure of refractory wall happens.***
Key words: Cylindrical Coordinate System, Temperature distribution, Stress distribution, Finite Difference Model

I. INRODUCTION

Furnace is a term used to identify a closed space where heat is applied to a body in order to raise its temperature. The source of heat may be fuel or electricity. Commonly, metals and alloys and sometimes non-metals are heated or melted in furnaces. The purpose of heating defines the temperature of heating and heating rate. Increase in temperature softens the metals. They become amenable to distortion. This relaxing occurs with or without a change in the metallic structure. Heating to lower temperatures (below the critical temperature) of the metal softens it by relieving the internal stresses. On the other hand, metals heated to temperatures above the critical temperatures leads to changes in crystal structures and recrystallization like annealing. Further some metals and alloys are melted, ceramic products vitrified, coals coked, metals like zinc are vaporized and many other processes are completed in Furnaces.
Induction melting and heating furnaces are widely used in the iron industry and steel industry for the casting of the different grades of cast iron products. Refractory wall of induction melting furnace is a key component which is used as insulation layer. It is made of ramming mass like silica, alumina, magnesia etc. The refractory wall is directly influenced by the thermal cycling of the high temperature molten iron in the furnace. Thermal fatigue failure is easy to happen for it because of the larger phase transformation thermal stresses and it has a shorter life. This can cause serious production accidents. Therefore, the service life problem of the refractory wall has always been a focus of attention in the application of this to the industry.
The research on the distribution of temperature and thermal stress with respect to time for the refractory wall will not only put foundation for the investigation on the thermal fatigue of this kind of parts under thermal fatigue condition of low cycle and high phase transition stresses but also offers effective control for thermal fatigue failure and provide basis for improvement of life span of these kind of parts.
Computational heat transfer, computational fluid dynamic analysis is done for induction melting furnace, refrigerator condenser, induction heating furnace using different numerical methods like finite volume method and finite element method by different researchers.
Here, Explicit Finite Difference Method is used to find out temperature and thermal stress variation with respect to time.

II. DEVELOPMENT OF FINITE DIFFERENCE MODEL

We have divided Induction Furnace Wall into a Nodal Network as shown in Fig. 1. It is divided into 24 nodes. We have derived Explicit Finite Difference Equations for all nodes as per the boundary conditions applied to it. The furnace wall is having thermal conduction heat transfer between different nodes. It is having atmospheric heat convection ha applied from top side of the furnace wall which is open to atmosphere. It is having heat convection from molten metal from inside which is hi. It is having heat convection ho from cooling water which is circulating outside the furnace wall.

To solve this advanced heat transfer problem of induction melting furnace wall which is made from Alumina Ramming Mass, the following initial and boundary conditions, material properties and basic assumptions are made:

A. Refractory Materials for induction melting furnace wall meets the basic assumptions in the science of mechanics.
B. Environmental Air Temperature is homogeneous at 27° C.
C. Ignore the influence of heat radiation.
D. Ignore the effect of gravity field on wall.
E. The surface of induction melting furnace wall is clean and clear.
F. The initial temperature of the induction melting furnace is set 27° C and it is agreement with the ambient temperature during solving the problem.
G. Heat convections from air, cooling water and molten metal are considered constant for this analysis.
H. Scarp raw material input inside furnace is considered uniform for our analysis.

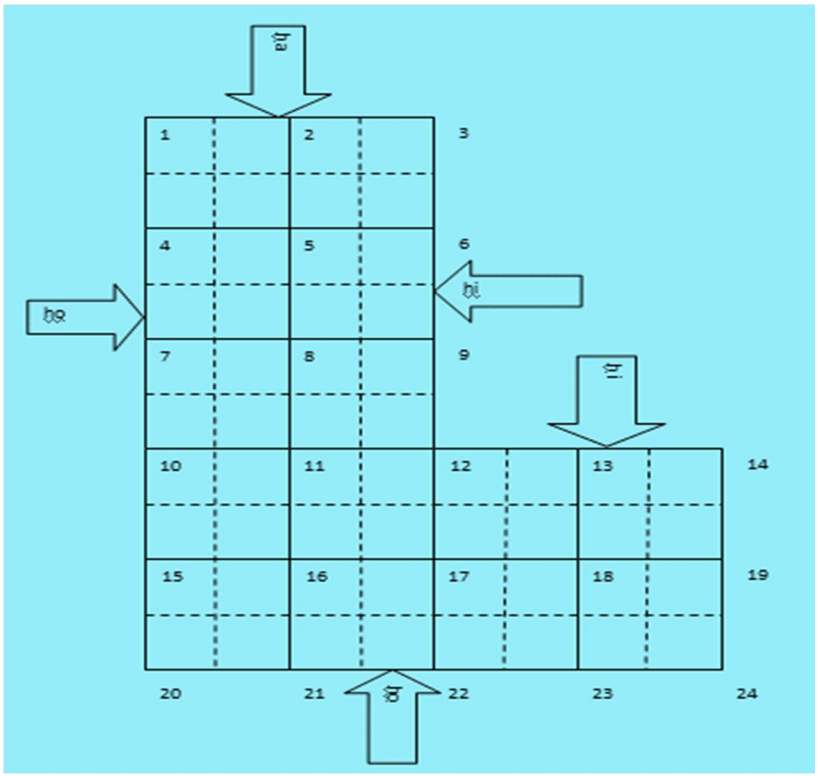

Fig.1. Nodal network for finite difference method

1) NODE: -1

$$T_1^{i+1} = \left((h_a \frac{\Delta x}{2}(T_\infty - T_1^i) + h_o \frac{\Delta y}{2}(T_\infty - T_1^i) + \pi k \Delta y \frac{T_2^i - T_1^i}{\ln\left(\frac{r_1}{r_2}\right)} + k\frac{\Delta x}{2}\frac{T_4^i - T_1^i}{\Delta y}\right)\frac{4\Delta t}{\rho C \Delta x \Delta y}\right) + T_1^i$$

T [1][i+1] = (((0.5*h $_a$*x*(T_o– T[1][i])) + (h_o*y*(T_a– T[1][i]/2) +(π*k*y*(T[2][i]-T[1][i])/ln(r_1/r_2)) +(0.5*k*x*(T[4][i]-T[1][i]/y))*((4*t)/(r*c*x*y)))+T[1][i];

2) NODE:-2

$$T_2^{i+1} = \left((h_a \Delta x (T_\infty - T_2^i) + \pi k \Delta y \frac{T_1^i - T_2^i}{\ln\left(\frac{r_1}{r_2}\right)} + \pi k \Delta y \frac{T_3^i - T_2^i}{\ln\left(\frac{r_2}{r_3}\right)} + k\Delta x \frac{T_5^i - T_2^i}{\Delta y}\right)\frac{2\Delta t}{\rho C \Delta x \Delta y}\right) + T_2^i$$

T[2][i+1]=(((h $_a$*x*(T_o – T[2][i]))+(π*k*y*(T[1][i]-T[2][i])/ln(r_1/r_2)+(π*k*Y*T[3][i]-T[2][i]/ In(r_2/r_3)+k*x*(T[5][i]-T[2][i])/y))*((2*t)/(r*c*x*y)))+T[2][i];

3) NODE:-3

$$T_3^{i+1}= (h_a\frac{\Delta x}{2}(T_\infty\text{-}T_3^{i})+h_i\frac{\Delta y}{2}(T_h\text{-}T_3^{i})+ \pi k\Delta y\frac{T_2^i-T_3^i}{\ln(\frac{r_2}{r_3})}+ k\frac{\Delta x}{2}\frac{T_6^i-T_3^i}{\Delta y}\Big)\frac{4\Delta t}{\rho C\Delta x\Delta y}\Big)+T_3^{i}$$

T [3][i+1] = (((h $_a$*x*(T$_o$ – T[3][i]*0.5) + (h$_i$ *y*(T$_h$ - T[3][i]*0.5)+(0.5*k*x*(T[6][i]-T[3][i]/y)+(π*k*y*(T[2][i]-T[3][i])/ln(r_2/r$_3$)))*((4*t)/(r*c*x*y)))+T[3][i];

4) NODE:-4

$$T_4^{i+4}= (h_o\Delta y\ (T_\infty\text{-}T_4^{i})+\pi k\Delta y\frac{T_5^i-T_4^i}{\ln(\frac{r_1}{r_2})}+k\frac{\Delta x}{2}\frac{T_1^i-T_4^i}{\Delta y}+k\frac{\Delta x}{2}\frac{T_7^i-T_4^i}{\Delta y}\Big)\frac{2\Delta t}{\rho C\Delta x\Delta y}\Big)+T_4^{i}$$

T [4][i+1] = (((h $_o$ *y*(T$_a$– T[4][i])) + (π*k*y*(T[5][i]-T[4][i])/ln(r_1/r$_2$)) + (0.5*k*x*(T[1][i]-T[4][i]/y) + (0.5*k*x*(T[7][i]-T[4][i])/y))*((2*t)/(r*c*x*y)))+T[4][i];

5) NODE:-5

$$T_5^{i+1}= ((\pi k\Delta y\frac{T_4^i-T_5^i}{\ln(\frac{r_1}{r_2})}+ \pi k\Delta y\frac{T_6^i-T_5^i}{\ln(\frac{r_2}{r_3})}+k\Delta x\frac{T_2^i-T_5^i}{\Delta y}+ k\Delta x\frac{T_8^i-T_5^i}{\Delta y}\Big)\frac{\Delta t}{\rho C\Delta x\Delta y}\Big)+T_5^{i}$$

T [5][i+1] = (((π*k*y*(T[4][i]-T[5][i])/ln(r_1/r$_2$)) + (π*k*y*(T[6][i]-T[5][i])/ln(r_2/r$_3$)) +(k*x*(T[2][i]-T[5][i]/y) +(k*x*(T[8][i]-T[5][i]/y))*((t)/(r*c*x*y)))+T[5][i];

6) NODE:-6

$$T_6^{i+1}= ((h_i\Delta y\ (T_h\text{-}T_6^{i}) +\pi k\Delta y\frac{T_5^i-T_6^i}{\ln(\frac{r_2}{r_3})}+k\frac{\Delta x}{2}\frac{T_3^i-T_6^i}{\Delta y}+k\frac{\Delta x}{2}\frac{T_9^i-T_6^i}{\Delta y}\Big)\frac{2\Delta t}{\rho C\Delta x\Delta y}\Big)+T_6^{i}$$

T [6][i+1] = (((h $_i$*y*(T$_h$– T[6][i])) + (π*k*y*(T[5][i]-T[6][i])/ln(r_2/r$_3$)) + (0.5*x*k*(T[3][i]-T[6][i]/y) + (0.5*k*x*(T[9][i]-T[6][i])/y))*((2*t)/(r*c*x*y)))+T[6][i];

7) NODE:-7

$$T_7^{i+7}= ((h_o\Delta y\ (T_\infty\text{-}T_7^{i}) + \pi k\Delta y\frac{T_8^i-T_7^i}{\ln(\frac{r_1}{r_2})} + k\frac{\Delta x}{2}\frac{T_4^i-T_7^i}{\Delta y} + k\frac{\Delta x}{2}\frac{T_{10}^i-T_7^i}{\Delta y}\Big)\frac{2\Delta t}{\rho C\Delta x\Delta y}\Big)+T_7^{i}$$

T [7][i+1] = (((h $_o$*y*(T$_a$– T[7][i])) + (π*k*y*(T[8][i]-T[7][i])/ln(r_1/r$_2$) + (k*0.5*x*(T[4][i]-T[7][i]/y) + (0.5*k*x*(T[10][i]-T[7][i])/y))*((2*t)/(r*c*x*y)))+T[7][i];

8) NODE:-8

$$T_8^{i+1}= ((\pi k\Delta y\frac{T_7^i-T_8^i}{\ln(\frac{r_1}{r_2})} + \pi k\Delta y\frac{T_9^i-T_8^i}{\ln(\frac{r_2}{r_3})} + k\Delta x\frac{T_5^i-T_8^i}{\Delta y} + k\Delta x\frac{T_{11}^i-T_8^i}{\Delta y}\Big)\frac{\Delta t}{\rho C\Delta x\Delta y}\Big)+T_8^{i}$$

T [8][i+1] = (((π*k*y*(T[7][i]-T[8][i])/ln(r_1/r$_2$)) +(π*k*y*(T[9][i]-T[8][i])/ln(r_2/r$_3$)) +(k*x*(T[5][i]-T[8][i])/y) + (k*x*(T[11][i]-T[8][i])/y)) *((t)/(r*c*x*y)))+T[8][i];

9) NODE:-9

$$T_9^{i+1}= ((h_i\Delta y\ (T_h\text{-}T_9^{i}) + \pi k\Delta y\frac{T_8^i-T_9^i}{\ln(\frac{r_2}{r_3})} + k\frac{\Delta x}{2}\frac{T_6^i-T_9^i}{\Delta y} + k\frac{\Delta x}{2}\frac{T_{12}^i-T_9^i}{\Delta y}\Big)\frac{2\Delta t}{\rho C\Delta x\Delta y}\Big)+T_9^{i}$$

T [9][i+1] = ((h$_i$*y*(T$_h$– T[9][i])) + (π*k*y*(T[8][i]-T[9][i])/ln(r_2/r$_3$)) + (k*0.5*x*(T[6][i]-T[9][i]/y) + (0.5*k*x*(T[12][i]-T[9][i])/y))*((2*t)/(r*c*x*y)))+T[9][i];

10) NODE:-10

$$T_{10}^{i+10}=\left((h_o\Delta y\,(T_\infty-T_{10}^{i})+\pi k\Delta y\frac{T_{11}^{i}-T_{10}^{i}}{\ln\left(\frac{r_1}{r_2}\right)}+k\frac{\Delta x}{2}\frac{T_{7}^{i}-T_{10}^{i}}{\Delta y}+k\frac{\Delta x}{2}\frac{T_{15}^{i}-T_{10}^{i}}{\Delta y}\right)\frac{2\Delta t}{\rho C\Delta x\Delta y}\right)+T_{10}^{i}$$

T [10][i+1] = (((h $_o$*y*(T_a– T[10][i])) + (π*k*y*(T[11][i]-T[10][i])/ln(r_1/r_2)) + (0.5*k*x*(T[7][i]-T[10][i]/y) + (0.5*k*x*(T[15][i]-T[10][i])/y))*((2*t)/(r*c*x*y)))+T[10][i];

11) NODE:-11

$$T_{11}^{i+1}=\left((\pi k\,\Delta y\frac{T_{10}^{i}-T_{11}^{i}}{\ln\left(\frac{r_1}{r_2}\right)}+\pi k\Delta y\frac{T_{12}^{i}-T_{11}^{i}}{\ln\left(\frac{r_2}{r_3}\right)}+k\Delta x\frac{T_{8}^{i}-T_{11}^{i}}{\Delta y}+k\Delta x\frac{T_{16}^{i}-T_{11}^{i}}{\Delta y}\right)\frac{\Delta t}{\rho C\Delta x\Delta y}\right)+T_{11}^{i}$$

T [11][i+1] = ((π*k*y*(T[10][i]-T[11][i])/ln(r_1/r_2)) + (π*k*y*(T[12][i]-T[11][i])/ln(r_2/r_3)) + (k*x*(T[8][i]-T[11][i])/y) + (k*x*(T[16][i]-T[11][i])/y))*((t)/(r*c*x*y)))+T[11][i];

12) NODE:-12

$$T_{12}^{i+1}=\left((h_i\frac{\Delta x}{2}(T_h-T_{12}^{i})+h_i\frac{\Delta y}{2}(T_h-T_{12}^{i})+\pi k\Delta y\frac{T_{11}^{i}-T_{12}^{i}}{\ln\left(\frac{r_2}{r_3}\right)}+\pi k\Delta y\frac{T_{13}^{i}-T_{12}^{i}}{\ln\left(\frac{r_3}{r_4}\right)}+k\frac{\Delta x}{2}\frac{T_{9}^{i}-T_{12}^{i}}{\Delta y}+\;k\Delta x\frac{T_{17}^{i}-T_{12}^{i}}{\Delta y}\right)\frac{4\Delta t}{\rho C\Delta x\Delta y}\right)+T_{12}^{i}$$

T [12][i+1] = (((0.5*h$_i$*x*(T_h– T[12][i])) + (0.5*h$_i$*y*(T_h– T[12][i])) + (π*k*y*(T[11][i]-T[12][i])/ln(r_2/r_3)) +(π*k*y*(T[13][i]-T[12][i])/ln(r_3/r_4)) + (0.5*k*x*(T[9][i]-T[12][i])/y) + (k*x*(T[17][i]-T[12][i])/y)*((4*t)/(3*r*c*x*y)))+T[12][i];

13) NODE:-13

$$T_{13}^{i+1}=\left((h_i\Delta x\,(T_h-T_{13}^{i})+\pi k\Delta y\frac{T_{12}^{i}-T_{13}^{i}}{\ln\left(\frac{r_3}{r_4}\right)}+\pi k\Delta y\frac{T_{14}^{i}-T_{13}^{i}}{\ln\left(\frac{r_4}{r_5}\right)}+k\Delta x\frac{T_{18}^{i}-T_{13}^{i}}{\Delta y}\right)\frac{2\Delta t}{\rho C\Delta x\Delta y}\right)+T_{13}^{i}$$

T [13][i+1] = (((h$_i$*x*(T_h– T[13][i])) + (π*k*y*(T[12][i]-T[13][i])/ln(r_3/r_4)) + (π*k*y*(T[14][i]-T[13][i])/ln(r_4/r_5)) + (k*x*(T[18][i]-T[13][i]/y)*((2*t)/(r*c*x*y)))+T[13][i];

14) NODE:-14

$$T_{14}^{i+1}=\left((h_i\frac{\Delta x}{2}(T_h-T_{14}^{i})+h_i\frac{\Delta y}{2}(T_h-T_{14}^{i})+\pi k\Delta y\frac{T_{13}^{i}-T_{14}^{i}}{\ln\left(\frac{r_4}{r_5}\right)}+k\frac{\Delta x}{2}\frac{T_{19}^{i}-T_{14}^{i}}{\Delta y}\right)\frac{4\Delta t}{\rho C\Delta x\Delta y}\right)+T_{14}^{i}$$

T [14][i+1] = (((0.5*h$_i$*x*(T_h– T[14][i])) +(0.5*h$_i$*y*(T_h– T[14][i])) + (π*k*y*(T[13][i]-T[14][i])/ln(r_4/r_5)) + (k*0.5*x*(T[19][i]-T[14][i]/y))*((4*t)/(r*c*x*y)))+T[14][i];

15) NODE:-15

$$T_{15}^{i+15}=\left((h_o\Delta y\,(T_\infty-T_{15}^{i})+\pi k\Delta y\frac{T_{16}^{i}-T_{15}^{i}}{\ln\left(\frac{r_1}{r_2}\right)}+k\frac{\Delta x}{2}\frac{T_{10}^{i}-T_{15}^{i}}{\Delta y}+k\frac{\Delta x}{2}\frac{T_{20}^{i}-T_{15}^{i}}{\Delta y}\right)\frac{2\Delta t}{\rho C\Delta x\Delta y}\right)+T_{15}^{i}$$

T [15][i+1] = (((h $_o$*y*(T_a– T[15][i])) + (π*k*y*(T[16][i]-T[15][i])/ln(r_1/r_2)) + (0.5*k*x*(T[10][i]-T[15][i]/y) + (0.5*k*x*(T[20][i]-T[15][i])/y))*((2*t)/(r*c*x*y)))+T[15][i];

16) NODE:-16

$$T_{16}^{i+1}=\left((\pi k\,\Delta y\frac{T_{15}^{i}-T_{16}^{i}}{\ln\left(\frac{r_1}{r_2}\right)}+\pi k\Delta y\frac{T_{17}^{i}-T_{16}^{i}}{\ln\left(\frac{r_2}{r_3}\right)}+k\Delta x\frac{T_{11}^{i}-T_{16}^{i}}{\Delta y}+k\Delta x\frac{T_{21}^{i}-T_{16}^{i}}{\Delta y}\right)\frac{\Delta t}{\rho C\Delta x\Delta y}\right)+T_{16}^{i}$$T [16][i+1] = ((π*k*y*(T[15][i]-T[16][i])/ln(r_1/r_2)) + (π*k*y*(T[17][i]-T[16][i])/ln(r_2/r_3)) + (k*x*(T[11][i]-T[16][i])/y) + (k*x*(T[21][i]-T[16][i])/y))*((t)/(r*c*x*y)))+T[16][i];

17) NODE:-17

$$T_{17}^{i+1}= \left(\left(\pi k\Delta y \frac{T_{16}^{i}-T_{17}^{i}}{\ln\left(\frac{r_2}{r_3}\right)}+ \pi k\Delta y \frac{T_{18}^{i}-T_{17}^{i}}{\ln\left(\frac{r_3}{r_4}\right)}+ k\Delta x \frac{T_{12}^{i}-T_{17}^{i}}{\Delta y} + k\Delta x \frac{T_{22}^{i}-T_{17}^{i}}{\Delta y}\right) \frac{\Delta t}{\rho C\Delta x\Delta y}\right)+T_{17}^{i}$$

T [17][i+1] = ((π*k*y*(T[16][i]-T[17][i])/ln(r_2/r_3)) +(π*k*y*(T[18][i]-T[17][i])/ln(r_3/r_4)) + (k*x*(T[12][i]-T[17][i])/y) + (k*x*(T[22][i]-T[17][i])/y))*((t)/(r*c*x*y)))+T[17][i];

18) NODE:-18

$$T_{18}^{i+1}= \left(\left(\pi k\Delta y \frac{T_{17}^{i}-T_{18}^{i}}{\ln\left(\frac{r_3}{r_4}\right)}+ \pi k\Delta y \frac{T_{19}^{i}-T_{18}^{i}}{\ln\left(\frac{r_4}{r_5}\right)}+ k\Delta x \frac{T_{13}^{i}-T_{18}^{i}}{\Delta y} + k\Delta x \frac{T_{23}^{i}-T_{18}^{i}}{\Delta y}\right) \frac{\Delta t}{\rho C\Delta x\Delta y}\right)+T_{18}^{i}$$

T [18][i+1] = ((π*k*y*(T[17][i]-T[18][i])/ln(r_3/r_4)) + (π*k*y*(T[19][i]-T[18][i])/ln(r_4/r_5)) + (k*x*(T[13][i]-T[18][i]/y) +(k*x*(T[23][i]-T[18][i]/y) *((t)/(r*c*x*y)))+T[18][i];

19) NODE:-19

$$T_{19}^{i+1}= \left(\left(h_i\Delta y\ (T_h\text{-}T_{19}^{i}) + \pi k\Delta y \frac{T_{18}^{i}-T_{19}^{i}}{\ln\left(\frac{r_4}{r_5}\right)}+ k\frac{\Delta x}{2} \frac{T_{14}^{i}-T_{19}^{i}}{\Delta y} + k\frac{\Delta x}{2} \frac{T_{24}^{i}-T_{19}^{i}}{\Delta y}\right) \frac{2\Delta t}{\rho C\Delta x\Delta y}\right)+T_{19}^{i}$$

T [19][i+1] = ((h_i*y*(T_h– T[19][i])) + (π*k*y*(T[18][i]-T[19][i])/ln(r_4/r_5)) + (k*0.5*x*(T[14][i]-T[19][i]/y) + (0.5*k*x*(T[24][i]-T[19][i]/y))*((2*t)/(r*c*x*y)))+T[19][i];

20) NODE:-20

$$T_{20}^{i+20}= \left(\left(h_o\frac{\Delta x}{2}\ (T_\infty\text{-}T_{20}^{i}) + \left(\left(h_o\frac{\Delta y}{2}\ (T_\infty\text{-}T_{20}^{i})+ \pi k\Delta y \frac{T_{21}^{i}-T_{20}^{i}}{\ln\left(\frac{r_1}{r_2}\right)}+ k\frac{\Delta x}{2} \frac{T_{15}^{i}-T_{20}^{i}}{\Delta y}\right) \frac{4\Delta t}{\rho C\Delta x\Delta y}\right)+T_{20}^{i}\right.\right.$$

T [20][i+1] = (((0.5*h_o*x*(T_a– T[20][i])) + (0.5*h_o*y*(T_a– T[20][i])) +(π*k*y*(T[21][i]-T[20][i])/ln(r_1/r_2)) +(0.5*x*k*(T[15][i]-T[20][i]/y))*((4*t)/(r*c*x*y)))+T[20][i];

21) NODE:-21

$$T_{21}^{i+1}= \left(\left(h_o\Delta x\ (T_\infty\text{-}T_{21}^{i}) + \pi k\Delta y \frac{T_{20}^{i}-T_{21}^{i}}{\ln\left(\frac{r_1}{r_2}\right)}+ \pi k\Delta y \frac{T_{22}^{i}-T_{21}^{i}}{\ln\left(\frac{r_2}{r_3}\right)}+ k\Delta x \frac{T_{16}^{i}-T_{21}^{i}}{\Delta y}\right) \frac{2\Delta t}{\rho C\Delta x\Delta y}\right)+T_{21}^{i}$$

T [21][i+1] = ((h_o*x*(T_a– T[21][i])) + (π*k*y*(T[20][i]-T[21][i])/ln(r_1/r_2)) + (π*k*y*(T[22][i]-T[21][i])/ln(r_2/r_3)) + (k*x*(T[16][i]-T[21][i]/y))*((2*t)/(r*c*x*y)))+T[21][i];

22) NODE:-22

$$T_{22}^{i+1}= \left(\left(h_o\Delta x\ (T_\infty\text{-}T_{22}^{i}) + \pi k\Delta y \frac{T_{21}^{i}-T_{22}^{i}}{\ln\left(\frac{r_2}{r_3}\right)}+ \pi k\Delta y \frac{T_{23}^{i}-T_{22}^{i}}{\ln\left(\frac{r_3}{r_4}\right)}+ k\Delta x \frac{T_{17}^{i}-T_{23}^{i}}{\Delta y}\right) \frac{2\Delta t}{\rho C\Delta x\Delta y}\right)+T_{22}^{i}$$

T [22][i+1] = ((h_o*x*(T_a– T[22][i])) + (π*k*y*(T[21][i]-T[22][i])/ln(r_3/r_4)) + (π*k*y*(T[23][i]-T[22][i])/ln(r_4/r_5)) + (k*x*(T[17][i]-T[22][i]/y))*((2*t)/(r*c*x*y)))+T[22][i];

23) NODE:-23

$$T_{23}^{i+1}= \left(\left(h_o\Delta x\ (T_\infty\text{-}T_{23}^{i}) + \pi k\Delta y \frac{T_{22}^{i}-T_{23}^{i}}{\ln\left(\frac{r_3}{r_4}\right)}+ \pi k\Delta y \frac{T_{24}^{i}-T_{23}^{i}}{\ln\left(\frac{r_4}{r_5}\right)}+ k\Delta x \frac{T_{18}^{i}-T_{23}^{i}}{\Delta y}\right) \frac{2\Delta t}{\rho C\Delta x\Delta y}\right)+T_{23}^{i}$$

T [23][i+1] = ((h_o*x*(T_a– T[23][i])) + (π*k*y*(T[22][i]-T[23][i])/ln(r_3/r_4)) + (π*k*y*(T[24][i]-T[23][i])/ln(r_4/r_5)) + (k*x*(T[18][i]-T[23][i]/y))*((2*t)/(r*c*x*y)))+T[23][i];

ISSN: 2321-9653; IC Value: 45.98; SJ Impact Factor: 7.177
Volume 8 Issue II Feb 2020- Available at www.ijraset.com

24) NODE:-24

$$T_{24}^{i+1} = \left(\left(h_o \frac{\Delta x}{2}\right)(T_\infty - T_{24}^{i}) + h_i \frac{\Delta y}{2}(T_h - T_{24}^{i}) + \pi k \Delta y \frac{T_{23}^{i} - T_{24}^{i}}{\ln\left(\frac{r_4}{r_5}\right)} + k\frac{\Delta x}{2}\frac{T_{19}^{i} - T_{24}^{i}}{\Delta y}\right)\frac{4\Delta t}{\rho C \Delta x \Delta y}\right) + T_{24}^{i}$$

T [24][i+1] = (((0.5*h $_o$*x*(T_a– T[24][i])) + (0.5*h_i*y*(T_h– T[24][i])) +(π*k*y*(T[23][i]-T[24][i])/ln(r_4/r_5)) +(0.5*k*x*(T[19][i]-T[24][i]/y))*((4*t)/(r*c*x*y)))+T[24][i];

III. PROGRAMMING & SOLUTION

With the help of a computer program we can solve the matrix created by finite difference equations for 24 nodes. We are using material properties and boundary conditions as given in Table 1. We can calculate temperature distribution and stress distribution with respect to time.

Table 1. Material Property and Boundary Conditions

Material Properties and Boundary Conditions for Silica Ramming Mass			Unit
1	Internal Film Co-efficient hi	200	W/m^2 K
2	External Film Co-efficient ho	40	W/m^2 K
3	Atmosphere Film Co-efficient ha	10	W/m^2 K
4	Density	3400	Kg/m^3
5	Time Interval Δt	10	Seconds
6	Thermal Conductivity k	2.6	W/m K
7	Temperature outside Furnace Wall	303	Kelvin
8	Temperature inside Furnace Wall	1873	Kelvin
9	Temperature of Air	303	Kelvin
10	Specific Heat	920	J/kg K
11	Elasticity Constant	220000	N/ m^2
12	Thermal Expansion Co-efficient	0.00000088	m/ K
13	Ultimate Stress	500	MPa

IV. RESULTS AND DISCUSSION

We can see from the Fig. 2 that maximum temperature is increasing from atmospheric temperature 300 K and reaches to maximum temperature 1787 K in 45 minutes and then starts reducing and reaches to 869 K in next 15 minutes. It again starts increasing and reaches to maximum 1787 K after 105 minutes and again starts reducing. There are 10 similar temperature cycles in one day.

We can see from the Fig. 3 that maximum thermal stress is increasing from initial condition 0 MPa and reaches to maximum stress 346 MPa in 45 minutes and then starts reducing and reaches to 168 MPa in next 15 minutes. It again starts increasing and reaches to maximum stress 346 MPa after 105 minutes and again it starts reducing. There are 10 similar thermal stress cycles in one day.

ISSN: 2321-9653; IC Value: 45.98; SJ Impact Factor: 7.177
Volume 8 Issue II Feb 2020- Available at www.ijraset.com

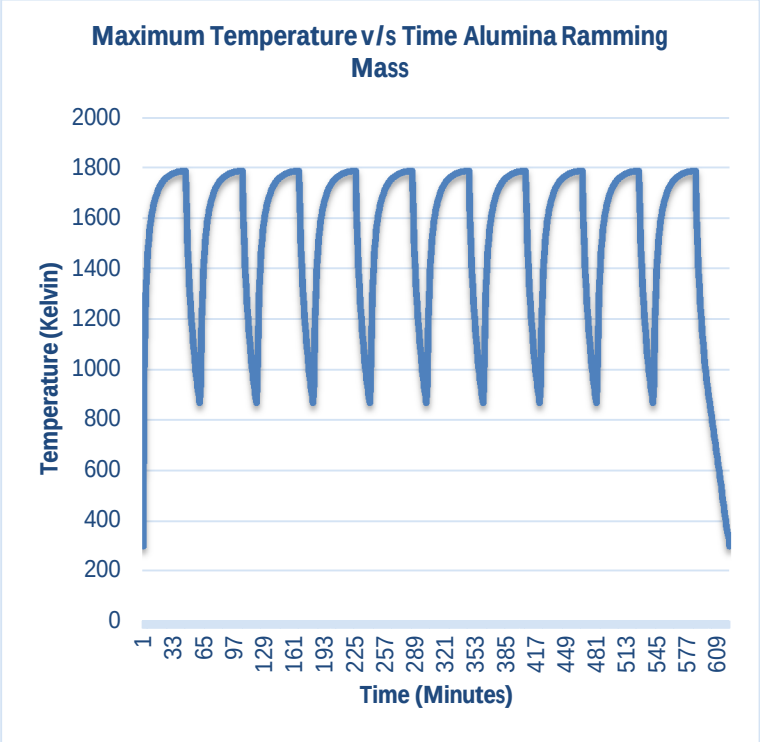

Fig. 2. Maximum Temperature v/s Time Graph for Alumina Ramming Mass

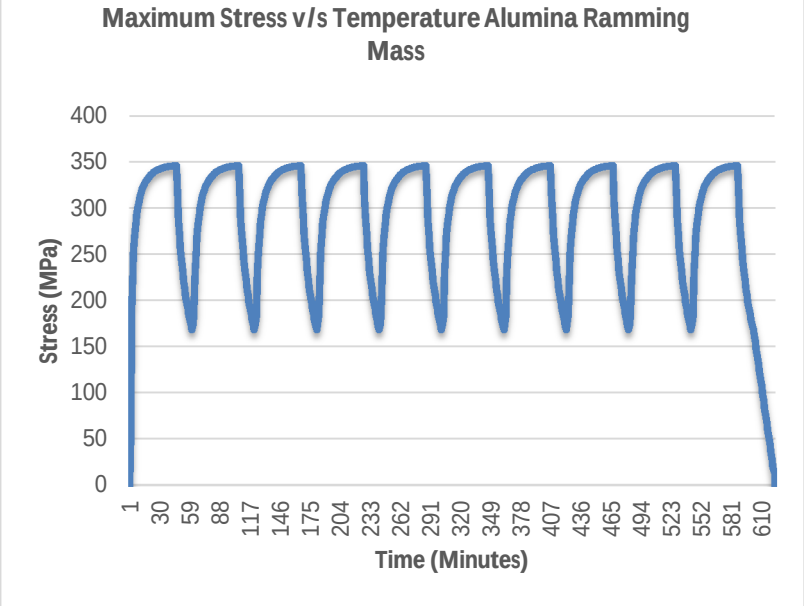

Fig. 3. Maximum Thermal Stress v/s Time Plot for Alumina Ramming Mass

V. CONCLUSION

Induction melting furnaces are highly used now- a-days for melting of different kinds of materials. We have found variation of maximum temperature and maximum stress with reference to time. From the graph, we can conclude that induction furnace wall which is made from alumina ramming mas is under the effect of low cycle thermal fatigue. The reason for its low life span is thermal fatigue behavior of its loading conditions.

VI. FUTURE SCOPE

This analysis can be utilized for prediction of life cycle of induction furnace wall which is made up of alumina based refractory materials. It can also be utilized to improve efficacy of furnace and optimization of wall thickness.

REFERENCES

[1] H, Kohne R, Nitsch J, Sprengel U, Solar thermal power plants for solar countries—technology, economics and market potential, Applied Energy 52(2–3), 1995; 165–83.
[2] Mancini TR, Kolb GJ, Chavez JM, Solar thermal power today and tomorrow, Mech. Engg., 116(8), 1994, 74–9.
[3] Ravi Kumar K, Reddy KS, Thermal analysis of solar parabolic trough with porous disc receiver. Applied Energy 86(9), 2009, 1804–12.
[4] Vanita Thakkar, Status of Parabolic Dish Solar Concentrators, International Journal of Enhanced Research in Science Technology & Engineering Vol. 2 Issue 6, June-2013, pp – 42-50
[5] S. A. Kalogirou, Solar thermal collectors and applications. Prgress in Energy and Combustion Science, 2004. 30: p. 231-295.
[6] Australian Energy Resource Assessment, Solar Energy.
[7] A. Sazena and S. Ghanshyam, Performance studies of a multipurpose solar Energy System for Remote areas. MIT International Journal of Mchanical Engineering, 2013. 3(1): p. 21-33.
[8] S. A. Kalogirou, Solar thermal collectors and applications. Prgress in Energy and Combustion Science, 2004. 30: p. 231-295.
[9] B.Sri Hari Priya, R. Santoshi Kumari, M. TukaramBai, V. Sridevi, Review on Water Desalination using Renewable Solar Energy. IJIRST –International Journal for Innovative Research in Science & Technology| Volume 2 | Issue 07 | December 2015.
[10] Philippe SCHILD, European Commission on Concentrated Solar Thermal Energy, Office CDMA 5-141, B-1049 Brussels.
[11] M. Ouannene, B. Chaouachi, S. Gabsi, design and realisation of a parabolic solar cooker. National School of Engineers of Gabes (E.N.I.G) - Omar Ibn El Khattab Street -6029 Gabes-Tunisia.
[12] Nirajkumar Mehta, (May 2012), Review on Computational Investigation on Different Kinds of Furnaces, International Conference on Emerging Technologies and Applications in Engineering, Technology and Sciences, Volume 3, pp 1 – 7.
[13] S. O. Jimoh (2013), analysis of the characteristics of the blast furnaces peripherical zone, international journal of science and technology research
[14] N C Mehta, Vipul B Gondaliya, Jayesh V Gundaniya, (February 2013), Applications of Different Numerical Methods in Heat Transfer - A Review, International Journal of Emerging Technology and Advanced Engineering, Volume 3, Issue 2, pp 363 – 368.
[15] Camilolezcano (2013), Numerical calculation of the recirculation factor in flameless furnaces, ISSN 0012-7353, pp 144-151.
[16] N C Mehta, Viral V Shiyani, Jemish R Nasit, (May 2013), Metal Forming Analysis, International Journal of Emerging Technology and Advanced Engineering, Volume 3, Issue 5, pp 190 - 196.
[17] Vipul Gondaliya, Mehul Pujara, Nirajkumar Mehta, (August 2013), Transient Heat Transfer Analysis of Induction Furnace by Using Finite Element Analysis, International Journal of Applied Research, Volume 3, Issue 8, pp 231 – 234.
[18] N C Mehta, Vasim G Machhar, Ravi K Popat, (October 2013), Thermal Fatigue Analysis of Induction Furnace Wall for Alumina ramming mass, International Journal of Science and Engineering Applications, Volume 2, Issue 10, pp 186 – 190, DOI: 10.7753/IJSEA0210.1002.
[19] Gaurav Kumar Thakur (2013), Analysis of fuel injection in blast furnaces with the help of CFD software approach, international journal of scientific and research publication, volume 3, issue 3, ISSN 2250-3153, page no-1-7.
[20] N C Mehta, Akash D Raiyani, Vikas R Gondalia, (February 2013), Thermal Fatigue Analysis of Induction Melting Furnace Wall for Silica ramming mass, International Journal of Emerging Technology and Advanced Engineering, Volume 3, Issue 2, pp 357 – 362.
[21] Vimal R Nakum, Kevin M Vyas, Niraj C Mehta, (April 2013), Research on Induction Heating - A Review, International Journal of Science and Engineering Applications, Volume 2, Issue 6, pp 141 – 144, DOI: 10.7753/IJSEA0206.1005.
[22] Andrey V Gil (2015), Research of integral parameters for furnaces of a circulating fluidized bed, EDP publication science, EPJ web of conference 82,01044, page no-01044-p.1-01044-p.5.
[23] Nirajkumar C Mehta, Dipesh D Shukla, Ravi K Popat, (December 2014), Optimization of Wall Thickness for Minimum Heat Loss for Induction Furnace by FEA, Indian Foundry Journal, Volume 60, No. 12, pp 19-25.
[24] Nirajkumar C Mehta, Dr. Dipesh D Shukla, Vishvash B Rajyaguru, (April 2015), Numerical Analysis of Furnace: Review, National Conference on Recent Research and Development in Core Disciplines of Engineering, Vadodara, Volume: 2, pp 1 -7.
[25] Nirajkumar C Mehta, Dr. Dipesh D Shukla, Vishvash B Rajyaguru, (April 2015), Thermal Fatigue Analysis of Induction Furnace Wall for Zirconia, National Conference on Recent Research and Development in Core Disciplines of Engineering, Vadodara, Volume: 2, pp 1 – 6.
[26] Nirajkumar C Mehta, Dr. Dipesh D Shukla, Pragnesh D Kandoliya, (April 2015), Comparison of Finite Difference Method and Finite Element Method for 2 D Transient Heat Transfer Problem, National Conference on Recent Research and Development in Core Disciplines of Engineering, Vadodara, Volume: 2, pp 1 – 10.
[27] Saheedlekangbad Mosi (2015), Effect of steel plants with three-phase induction furnaces on power distribution quality of the existing 33kv network in Nigeria, advance in science and technology research journal, volume 9, no.27, pages 1-10.
[28] Nirajkumar C Mehta, Dr. Dipesh D Shukla, (June 2015), Thermal Fatigue Analysis of Induction Furnace Wall for Magnesia Ramming Mass, ASME 2015 Applied Mechanics and Materials Conference, At Seattle, Washington, United States of America, Volume: 12, pp 1 – 6.
[29] Nirajkumar C Mehta, Dr. Dipesh D Shukla, Pragnesh D Kandoliya, (December 2016), Advanced Mathematical Modeling of Heat Transfer in Induction Furnace Wall of Zirconia, International Journal of Engineering Research and Technology, Volume 5, Issue 10, pp 176 – 181, DOI: 10.17577/IJERTV5IS120128
[30] Nirajkumar C Mehta, Dr. Dipesh D Shukla, Pragnesh D Kandoliya, (December 2016), Advanced Heat Transfer Analysis of Alumina Based Refractory Wall of Induction Furnace, National Conference on Emerging Trends in Engineering, Volume 1, pp 1 – 6.
[31] Piotr Bulinski (2016), coupled numerical model of metal melting in an induction furnace: sensitivity analysis and validation of model, Silesian university of technology, institute of thermal technology and Silesian university of technology, department of industrial informatics, ISSN 0033-2097

[32] Mirko Filipponi (2016), thermal analysis of an industrial furnace, MDPI Energies, 2016, 9, 833, 1-30.
[33] Prof. Nirajkumar C. Mehta, Dr. Dipesh D. Shukla, (December 2017) Mathematical Modelling for Life Cycle Forecasting of Zirconia Based Furnace Wall, International Journal of Advance Research and Innovative Ideas in Education, IJARIIE, ISSN(O)-2395-4396, Vol-3 Issue-4 2017, pp 796-807.
[34] Nirajkumar C Mehta, Dr. Dipesh D Shukla, Stress analysis of induction furnace wall for magnesia ramming mass, Journal of Metallurgy and Materials Science, Volume: 59, Issue: 2, pp. 85-110, Print ISSN: 0972-4257. Online ISSN: 0974-1267, November 2017.
[35] Nirajkumar C Mehta, Dr. Dipesh D Shukla, Comparison of Life Cycle for Various Refractory Materials of Induction Melting Furnace Wall under Thermal Fatigue Loading Conditions", International Journal of Advance Engineering and Research Development, e-ISSN (O): 2348-4470, p-ISSN (P): 2348-6406, Volume 5, Issue 01, January 2018.
[36] Patil Kaushal, Makwana Arjunsinh, Arab Mohammadazhar, Nirajkumar C Mehta, "Mathematically Advanced Computational Heat Transfer Analysis of Cylindrical and Spherical Induction Furnaces: Review", International Journal of Advance Engineering and Research Development, e-ISSN (O): 2348-4470, p-ISSN (P): 2348-6406, Volume 5, Issue 02, February 2018.
[37] Ronik Varia, Sachin Vasani, Rahul Varma, Dr. Nirajkumar C Mehta, "Review of Solar Heating Furnace Development", International Journal of Advance Engineering and Research Development, e-ISSN (O): 2348-4470, p-ISSN (P): 2348-6406, Volume 5, Issue 03, March -2018.
[38] Rahul Waghela, Shreyas Parmar, Susmit Vasava, Dr. Nirajkumar C Mehta, "Review of Refractory Materials for Innovative Investigation and Testing", International Journal of Advance Engineering and Research Development, e-ISSN (O): 2348-4470 p-ISSN (P): 2348-6406, Volume 5, Issue 03, March -2018.

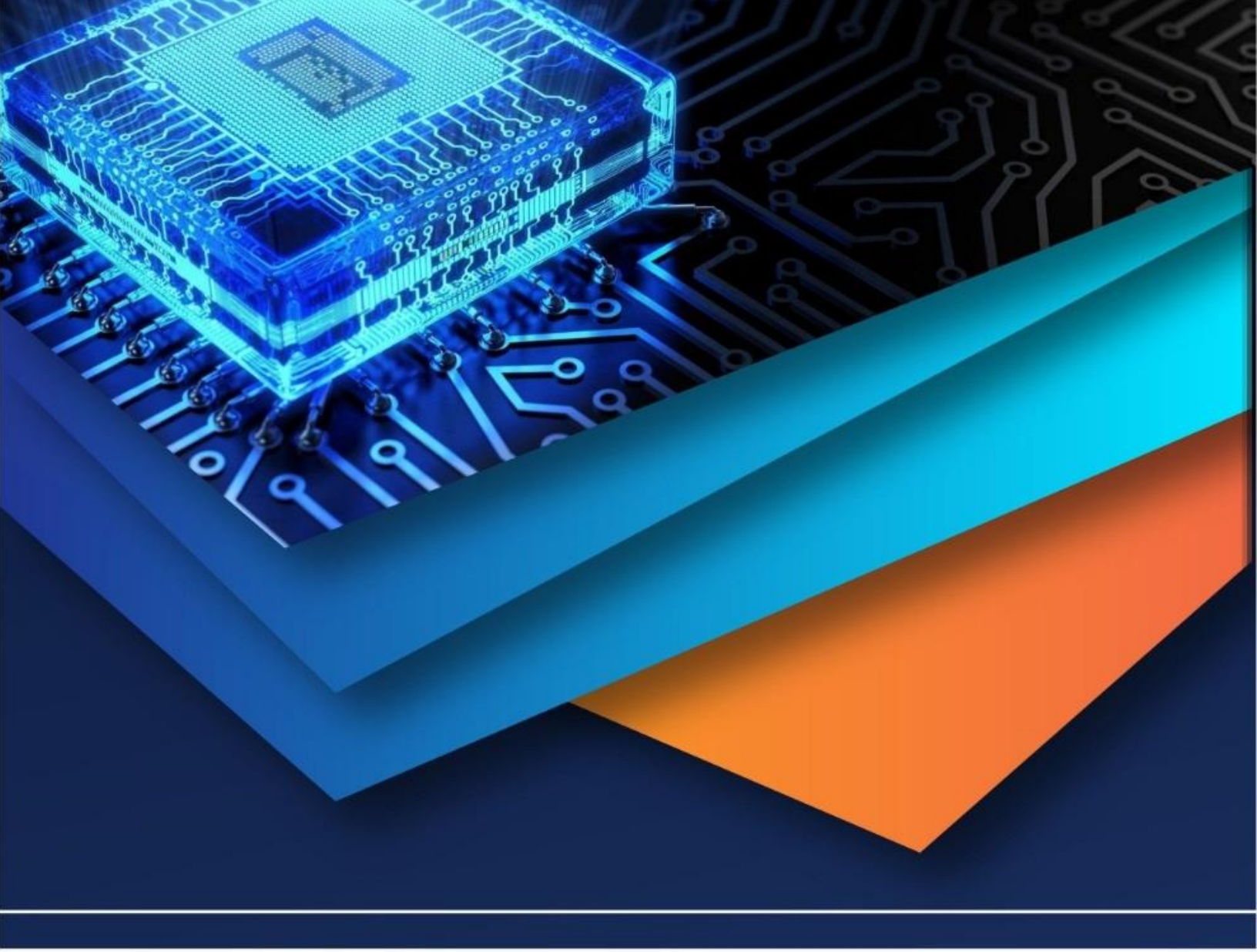

10.22214/IJRASET

45.98

IMPACT FACTOR: 7.129

IMPACT FACTOR: 7.429

INTERNATIONAL JOURNAL FOR RESEARCH

IN APPLIED SCIENCE & ENGINEERING TECHNOLOGY